

Free Flight Experiment Investigation of AOA Effect on Cone Boundary Layer Transition at Mach 6



Zonghao Wang, Sen Liu, and Jie Huang

Abstract To investigate the angle of attack (AOA) effect of hypersonic boundary layer transition on slightly blunted cone, China Aerodynamics Research and Development Center has conducted a series of ballistic free flight experiments on 5° half angle circular cones. The projectile is 110 mm long with surface roughness between $0.46 \mu\text{m}$ and $0.77 \mu\text{m}$. Six shots were taken under Mach 6 and separated unit Reynolds numbers, and the AOA varied between 0.2° and 7.9° . Results showed that the transition shifted upward to the nose tip on the leeside and afterward to the bottom on the windside within small AOA of less than 3° . When the angle got further increased, the moving direction of the transition on the windside reversed toward the nose tip but will not exceed the leeside in present results with nose tip radius of less than 0.4 mm. The transition Reynolds number without AOA was about 4.7×10^6 , and there was a noticeable decrement with AOA, which may relate with both pressure gradient and wall heating difference.

1 Introduction

Boundary-layer transition has always been hotspot of aerodynamic theory and experimental research, because of the important effects of boundary-layer to wide range of aerodynamic problems, especially for hypersonic vehicles. Since the famous Reynolds' water tube test in 1983, which found laminar and turbulence, researches on transition problems never stopped. For low-speed flow, semi-engineer method based on linear stability theory (LST) can predict the transition well. However, for supersonic and hypersonic flow, strong compression, high temperature, ablation, and real-gas effect make the boundary layer flow extremely complex. On one side, the environment disturbance differences reduce the ground test accuracy, and on the other side, most of the measurement technologies become useless or

Z. Wang · S. Liu (✉) · J. Huang

Hypervelocity Aerodynamics Institute, China Aerodynamics Research and Development Center, Miayang, People's Republic of China

e-mail: liusen@cardc.cn

© Springer Nature Switzerland AG 2019

A. Sasoh et al. (eds.), *31st International Symposium on Shock Waves 2*,
https://doi.org/10.1007/978-3-319-91017-8_117

931

unreliable in hypersonic condition. That is why the test results of a circular cone model, which is simple in shape but complicated in transition phenomena, differ from one facility to another.

For the effect of AOA, most present research results show that transition moves toward the nose tip on the leeside and moves opposite direction on the windside [1–8], while other tests show transition reverse [9–14]. This reveals the complexity of transition experiments, especially for blunted cone, and how to obtain consistent and reliable data becomes very important. Fly test is ideal, but it costs a lot and the test cycle is long. As a compromise, free flight test in ballistic range presents a new efficiency and effective approach.

Ballistic range, different from other wind tunnels, avoids the influence of support structures and background noise. The projectiles, accelerated to hypervelocity by a two-stage light-gas gun, fly freely in the test chamber, where the wall to stagnation temperature ratio and real-gas effect can be the same as the real flight. Recently, CARDC upgraded the shadowgraph imaging system of its ballistic range and applied in boundary layer flow visualization [15]. This paper will present a preliminary AOA effect study on circular cone at Mach 6 and try to improve the understanding of hypersonic boundary layer transition by qualitative and quantitative analysis.

2 Experiment Method

The experiment was carried out in the aerophysics range of Hypervelocity Aerodynamics Institute, CARDC. This facility consists of launch system, measurement system and test chamber, shown in Fig. 1. The launch system is a two-stage light-gas gun with 28 mm launch tube and maximum 7.2 km/s launch velocity. The measurement system contains three laser detect devices for velocity measurement, a set of high-resolution shadowgraph imaging station, and a central computer. The test chamber can simulate a flight environment of up to 60 km atmosphere by changing the vacuum level.

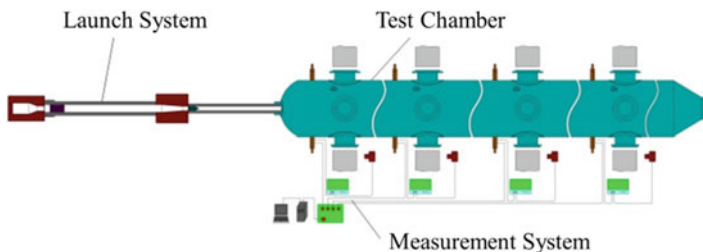


Fig. 1 Schematic diagram of CARDC aerophysics range

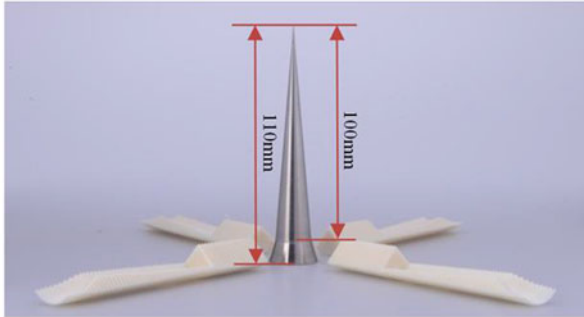


Fig. 2 The cone model and sabot

The 5° half angle circular cone model and sabot are shown in Fig. 2. It is about 110 mm long with skirt, and the radius of the nose tip is under 0.4 mm. It is made of steel and weight around 79 g. The surface roughness is between $0.46 \mu\text{m}$ and $0.77 \mu\text{m}$. The projectile must stand high acceleration load in the launch tube. Own to the soft launch technology [17], the launch load was notably reduced, and the successful launch rate was improved.

Mach number and Reynolds number are mainly simulated by controlling launch velocity and environment pressure separately in the ballistic range test. The Mach number is selected as 6 which is equal to about 2 km/s at the normal temperature.

3 Test Result

The conditions and results, including 6 shots, are shown in Table 1. The transition point X stands for the coordinate value of x axis started from the nose of the model. The tests were carried out under room temperature, and the wall to stagnation temperature ratio T_w/T_0 was about 0.12. The transition Reynolds number is defined as $Re_{tr} = X \times Re_\infty/L$. Test ZL-15, ZL-16, and ZL-29 had almost the same unit Reynolds number of about $6.5 \times 10^7 \text{ m}^{-1}$, while the other three tests had a higher unit Reynolds number of about $8.5 \times 10^7 \text{ m}^{-1}$, and their transition points were relatively earlier than the former group.

Figures 3 and 4 showed the shadowgraph images of test ZL-13 and ZL-30. They had nearly the same unit Reynolds number but different AOA of 7.9° and 0.2° separately. There were vast of spokewise acoustic waves, which were induced by turbulence, among the main shock and the cone surface. The pressure gradient from the windside to the leeside may cause cross flow and made the thickness of the boundary layer on the leeside greater than the windside. The transition points on both sides of the cone seemed equal in test ZL-30 as the cone flew with almost zero AOA. Turbulent spots and intermittent turbulence can be seen on the surface of the model.

Table 1 Test conditions and results

	Nose tip radius R (mm)	Ma _∞	Re _∞ /L (m ⁻¹)	AOA (deg)	Transition point X (mm)		Re _{tr}
					Windside	Leeside	
ZL-13	0.25	5.77	8.56×10^7	7.9	30	13	2.57×10^6
ZL-15	0.31	5.80	6.52×10^7	8.5	47	18	3.06×10^6
ZL-16	0.18	5.83	6.82×10^7	2.3	76	66	5.18×10^6
ZL-29	0.33	5.65	6.48×10^7	2.6	68	64	4.41×10^6
ZL-30	0.24	5.76	8.82×10^7	0.2	53	53	4.67×10^6
ZL-35	0.16	5.72	8.75×10^7	1.2	55	44	4.81×10^6
							1.11×10^6
							1.17×10^6
							4.50×10^6
							4.15×10^6
							4.67×10^6
							3.85×10^6

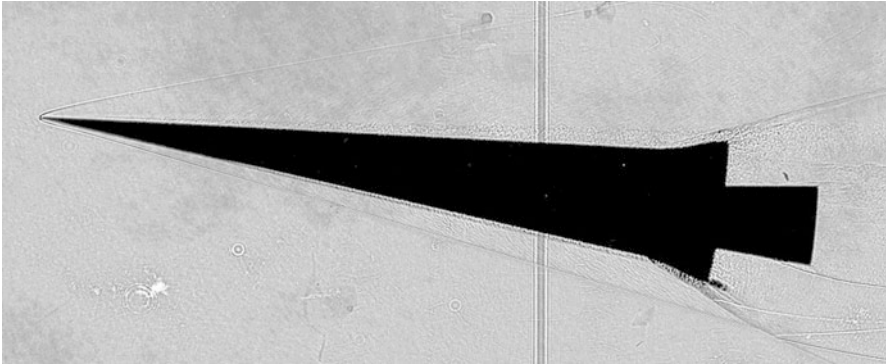


Fig. 3 The shadowgraph image of test ZL-13 ($Ma = 5.77$, $Re/L = 8.56 \times 10^7 \text{ m}^{-1}$, $\alpha = 7.9^\circ$)

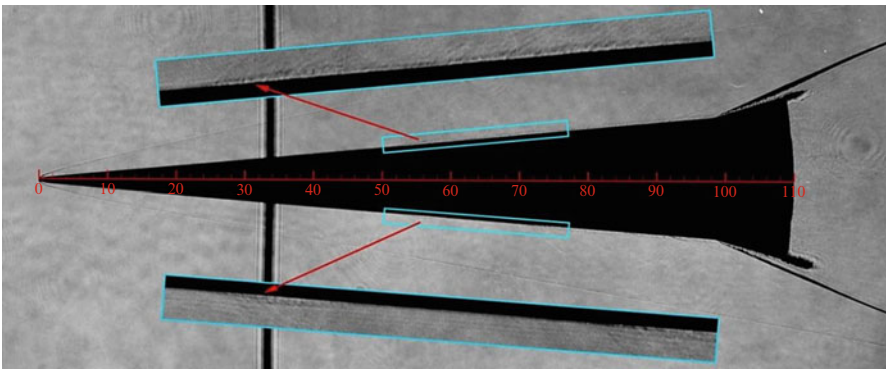


Fig. 4 The shadowgraph image of test ZL-30 ($Ma = 5.76$, $Re/L = 8.82 \times 10^7 \text{ m}^{-1}$, $\alpha = 0.2^\circ$)

There were vortices in the transition and turbulent area of the boundary layer, and they presented gray level changes in the image. The eddy scale distribution of the boundary layer was computed by FFT spectrum analysis, and it reflected the transition process from laminar to turbulence clearly. As an example, Fig. 5 shows bar charts of the eddy scale distribution on the windside and leeside of the cone of test ZL-30. In the laminar flow area, the eddy scale is under 0.2 mm with small fluctuation. At the transition point, one or more sharp bars stand out, and that corresponds to the turbulent spots. Some re-laminar areas between turbulent spots could be identified too. According to the eddy scale distribution, the transition could be located accurately.

The transition points on both leeside and windside of each test were compared in Fig. 6. Higher unit Reynolds number led to earlier transition. The transition shifted upward on the leeside and afterward on the windside within small AOA of less than 3° . When the angle gets further increased, the moving direction of the transition on the windside reversed toward the nose tip but will not exceed the leeside in the present results with nose tip radius of less than 0.4 mm.

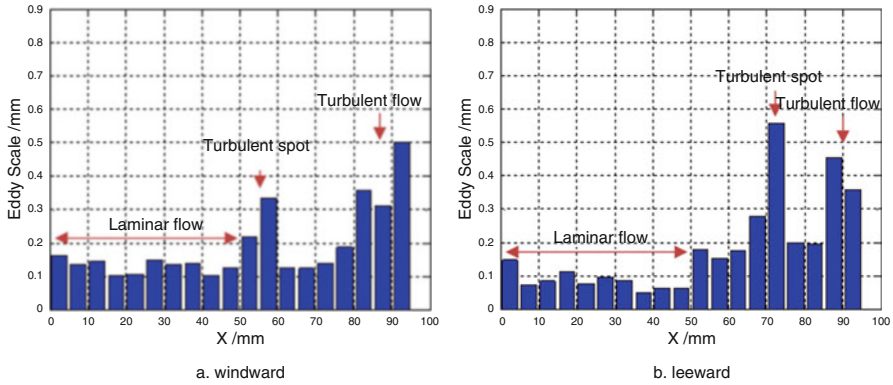


Fig. 5 The eddy scale distribution on the model of test ZL-30

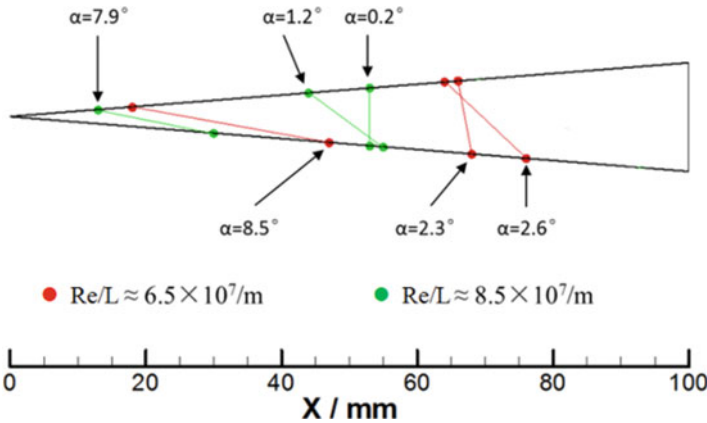


Fig. 6 Distribution of the transition point of different AOA and unit Reynolds number

For the slightly blunted cone, the main shock can be assumed to be stuck to the wall; therefore, it is easy to calculate the local parameters of basic flow theoretically. It seems the flow on the windside had a higher enthalpy and lower Mach number, and that resulted in unbalance transition on the cone’s surface with AOA.

4 Discussion

Some references ascribed the moving direction reverse of the transition to the crossflow increased by AOA. It is doubtful why there are so many differences between results of different facilities. At least, the crossflow effect is not the only mechanism to dominate transition process.

It is generally recognized that wind tunnel transition occurred at lower Reynolds numbers than in flight due to wind tunnel noise. However, the transition test result comparison of HiFIRE-1 on ground and in flight showed that there was noticeable decrement in transition Reynolds number with AOA from 5° to 13° , even in some case, wind tunnel windward transition occurred at a higher Reynolds number than in flight [18]. Ballistic range test also showed same differences in transition Reynolds number between small and big AOA.

It is noticed that there is a non-negligible change of wall to stagnation temperature ratio between wind tunnel ($T_w/T_0 = 0.56$) and in flight ($T_w/T_0 = 0.18$ for HiFIRE-1 fly test and $T_w/T_0 = 0.12$ for ballistic range test). Therefore, the destabilizing effects of wall cooling may outweigh the effect of background noise and play an important role in the transition problems. A recent paper of Tsinghua University reported that favorable pressure gradient will stabilize the first and second unsteady modes; however, a new mode may arise when wall heating added in the high-speed boundary layer [19]. This theory may help to study the AOA effect to the cone transition in further research.

5 Conclusion

The cone has a simple shape but quite complicated transition phenomenon in hypersonic flow. To investigate the AOA effect to the slightly blunted circular cone, CARDIC carried out a series of free flight test in the ballistic range.

Results showed that the transition location shifted upward on the leeside and afterward on the windside within small AOA. When the angle gets further increased, the moving direction of the transition on the windside reversed toward the nose tip but will not exceed the leeside in present results with nose tip radius of less than 0.4 mm. There is noticeable decrement in transition Reynolds number with AOA, which may related with both pressure gradient and wall heating. Further theoretical and experimental research is necessary.

Acknowledgments This work was supported by National Program on Key Research Project (Grant No. 2016YFA0401201).

References

1. E.J. Softley, Boundary layer transition of hypersonic blunt, slender cones, AIAA Paper 69-0705 (1969)
2. V. Dicristina, Three-dimensional laminar boundary layer transition on a sharp 8-deg. Cone at Mach 10. AIAA J. **8**(5) (1970)
3. M.C. Fischer, An experimental investigation of boundary layer transition on a 10-deg Half-angle cone at Mach 6.9, NASA TN-D-5766 (1970)

4. L.E. Sakell, *An Experimental Investigation of Boundary Layer Transition over Three Axially Symmetric Bodies at $M_\infty=6.0$* . Ph.D Thesis, New York University, New York (1972)
5. J.F. Muir, A.A. Trujillo, *Experimental Investigation of the Effects of Nose Bluntness, Free-Stream Unit Reynolds Number, and Angle of Attack on Cone Boundary Layer Transition at a Mach Number of 6*, AIAA Paper 72-216 (1972)
6. K.F. Stetson, Mach 6 experiments of transition on a cone at angle of attack. *J Spacecr.* **19**(5) (1982)
7. K.F. Stetson, E.R. Thompson, J.C. Donaldson, L.G. Siler, Laminar boundary layer stability experiments on a cone at Mach 8 part 3 sharp cone at angle of attack. AIAA Paper, 85-0492 (1985)
8. J. Perraud, D. Arnal, L. Dussillols, F. Thivet, Studies of laminar turbulent transition in hypersonic boundary layers at ONERA, in *European Symposium on Aerothermodynamics for Space Vehicles*, 1998
9. A. Martellucci, R.S. Neff, W.H. Truelli, An experimental investigation of boundary layer transition on a cone at angle of attack, NASA TR-69-0383 (1969)
10. V. DiCristina, Three-dimensional laminar boundary-layer transition on a sharp 8° cone at Mach 10. *AIAA J.* **8**(5) (1970)
11. J.F. Muir, A.A. Trujillo, Experimental investigation of the effects of nose bluntness, free-stream unit Reynolds number and angle of attack on cone boundary layer transition at a Mach number of 6, AIAA Paper 72-0216 (1972)
12. L.E. Sakell, *An experimental investigation of boundary layer transition over three axially symmetric bodies at Mach 6*, Ph.D. Thesis, New York University, School of Engineering and Science, (1972)
13. M.R. Malik, Numerical method for hypersonic boundary layer stability. *J. Comput. Phys.* **86** (1990)
14. J.E. Gronvall, H.B. Johnson, G.V. Candler, Hypersonic three-dimensional boundary layer transition on a cone at angle of attack. AIAA Paper, 2011-3561 (2011)
15. Z. Wang, S. Liu, A. Xie, J. Huang, Shadowgraph imaging and post-processing for hypersonic boundary layer transition in ballistic range, in *13th Asian Symposium of Visualization*, 154 (2015)
16. S.A. Stanfield, R.L. Kimmel, D. Adamczak, Boundary-layer transition experiment during reentry of HIFiRE-1. *J. Spacecr. Rocket.* **52**(3) (2015)
17. S.-c. Liang, J. Huang, Y. Li, et al., The effect of waves rupture diaphragm on acceleration loads of projectile. *Proc. Inst. Mech. Eng. Part G: J. Aerosp. Eng.* **228**(10) (2014)
18. S.A. Stanfield, R.L. Kimmel, D. Adamczak, et al., Boundary-layer transition experiment during reentry of HIFiRE-1. *J. Spacecr. Rocket* **52**(3) (2015)
19. J. Ren, S. Fu, *Instability of hypersonic boundary layer is caused by favorable pressure gradient and wall-heating*, AIAA Paper 2017-2134 (2017)